

Variability and uncertainty of meridional transports in the South Atlantic as estimated from Argo and altimetry

Claudia Schmid (Physical Oceanography Division, NOAA/AOML; Claudia.Schmid@noaa.gov)

1. Introduction

An analysis of the transports of the Atlantic Meridional Overturning Circulation (AMOC) in the subtropical South Atlantic is performed based on three-dimensional velocity fields derived from Argo data and AVISO sea surface heights. The main challenges are the under-sampling of the western boundary currents by the Argo array as well as the typical profiling depth of the Argo floats, which is about 2000m. The focus will therefore be on estimating transport in the upper branch of the AMOC both directly from the velocity field in the upper 2000m as well as from full depth profiles which are obtained by padding the profiles with climatological fields below 2000m. The determination of the uncertainty of the transports derived from the observations is done by sub-sampling the output fields from a numerical model to match the availability of observations and using climatology in the deeper layers. A statistical analysis of the actual AMOC transports in the model with the estimated ones will result in a measure of the uncertainty associated with the used method.

2. Estimating the Velocity - Data and Methodology

The Argo array is a global set of more than 3,000 free-drifting floats that sample the upper ocean to a maximum pressure level of 2000 dbar. Schmid (2014) developed a procedure to obtain monthly three-dimensional fields of absolute geostrophic velocities from Argo and altimeter data (AVISO) in the upper 2000 dbar. An updated version of the previous data set is based on 66,264 profiles of temperature and salinity collected in the South Atlantic in the years 2000 to 2013. The approach is based on correlating the dynamic height from Argo floats with the sea surface height from AVISO, with the goal to generate synthetic dynamic height profiles with better spatial and temporal coverage than could be achieved using only the in situ observations. Monthly mean dynamic height fields covering the period March 2000 to August 2013 are used to calculate the relative geostrophic velocities on a 0.5° longitude by 0.5° latitude grid from 5°S to 50°S . Subsurface velocities are estimated by using trajectory data from 801 Argo and WOCE floats (Dec. 9, 1992 to Feb. 20, 2014) whenever they drifted in the pressure range of 800 to 1100 dbar. They and the associated pressures are used to derive monthly mean fields of the subsurface velocity which in turn are used to estimate the absolute geostrophic velocity (Schmid, 2014). If no monthly mean subsurface velocity is available at a given grid point, then the climatological velocity is used. Finally, the Ekman velocity (using NCEP reanalysis 2 winds) is added.

The climatological field captures the Brazil and Malvinas Current in the confluence region near 40°S at the western boundary, the Benguela Current near the eastern boundary, the Agulhas Current and the meander of the Agulhas Return Current south of Africa (Fig. 1a). Similarly, the cross section at 35°S (Fig. 1b) shows the vertical extent of the Brazil Current at the western boundary and the Benguela Current at the eastern boundary.

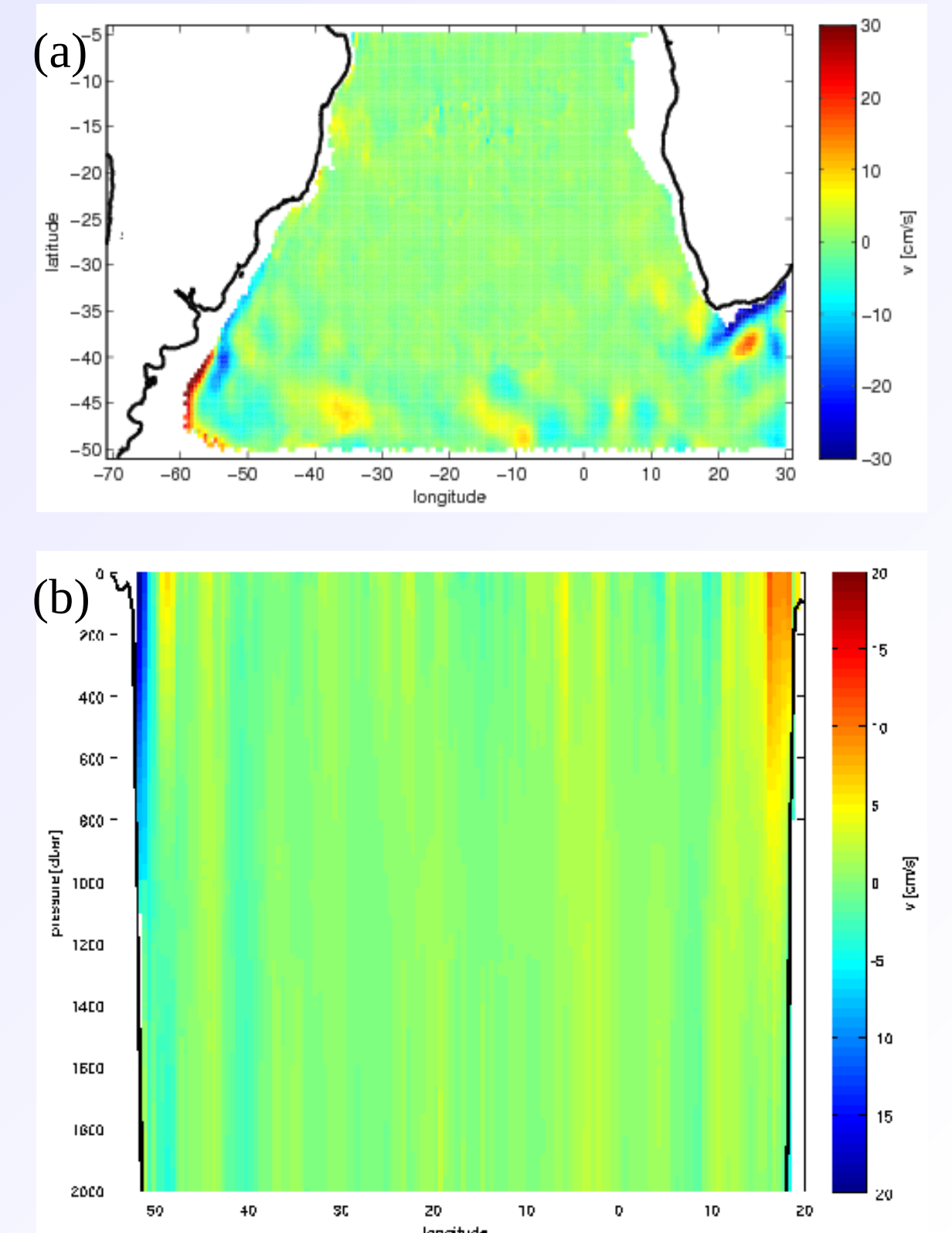


Fig. 1: Meridional adjusted geostrophic velocity (a) at 500 dbar. (b) at 35°S .

2. MOC Transport at 35S

The MOC transports are estimated by combining the velocity fields with gridded sections of the temperature and salinity derived from Argo and are padded with the hydrography from World Ocean Atlas 2013. The approach is similar to that used by Baringer and Garzoli (2007), with the main difference that the barotropic component is derived from the subsurface drift of floats. Mass conservation was applied to the transport estimates, and a correction based on a salt flux through the Bering Strait of $-26.7 \times 10^6 \text{ kg/s}$ was used (Coachman & Aagard, 1988). Figure 2 shows estimates from the Argo&SSH product (Schmid, 2014), the AX18 XBT sections and the OFES model.

The linear relationship between the volume transport of the MOC and the MOC heat transport is apparent in all three sets of results. The scatter plots comparing the heat transport of the MOC with the heat transports along the boundaries (in the upper 800m) as well as the interior (full depth) do not reveal a clear relationship between these quantities and the MOC heat transport. However, it is obvious that the interior heat transport contributes significantly to the overall heat transport of the MOC.

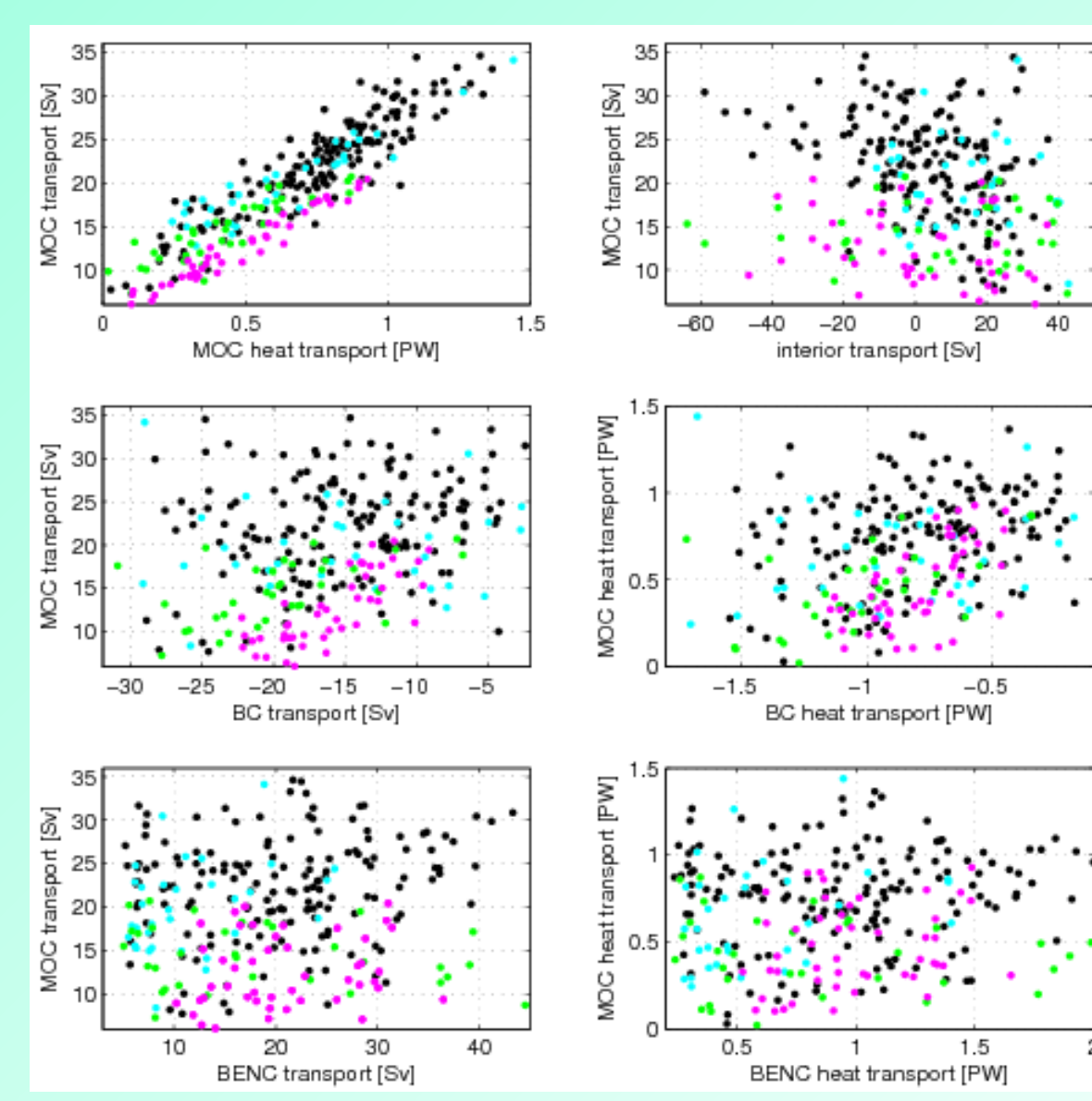


Fig. 2: MOC transports and their relationships to transports in the Brazil Current (BC), Benguela Current (BENC) and the interior. Black dots: from Argo&SSH (35°S), cyan: AX18 (nominally 35°S), magenta: NCEP GODAS (35°S). [units: $1 \text{ Sv} = 10^6 \text{ m}^3 \text{ s}^{-1}$, $1 \text{ PW} = 10^{15} \text{ Watt}$]

3. Impact of sub-sampling on MOC Transport

Monthly mean temperature, salinity and velocity fields from global HYCOM/NCODA Global Analysis (<http://hycom.org/dataserver/glb-analysis>, GLBa0.08, experiments 90.6, 90.8 and 90.9) are used to derive the MOC transport once at full zonal resolution (0.08°) and once using the same zonal resolution as the gridded velocity fields (0.5°). This simplified approach reveals that the transport based on the coarser resolution are about 2 Sv lower than those based on the full resolution. This difference is smaller than the standard deviation of the monthly means derived from 4 years of model fields. A significant portion of this difference is likely to be attributable to the poorer representation of the boundary currents, particularly the Brazil Current in the estimate derived with the coarser resolution fields.

Plans for the future include: using different models and model runs; sub-sampling with an approach that reflects the in situ sampling density.

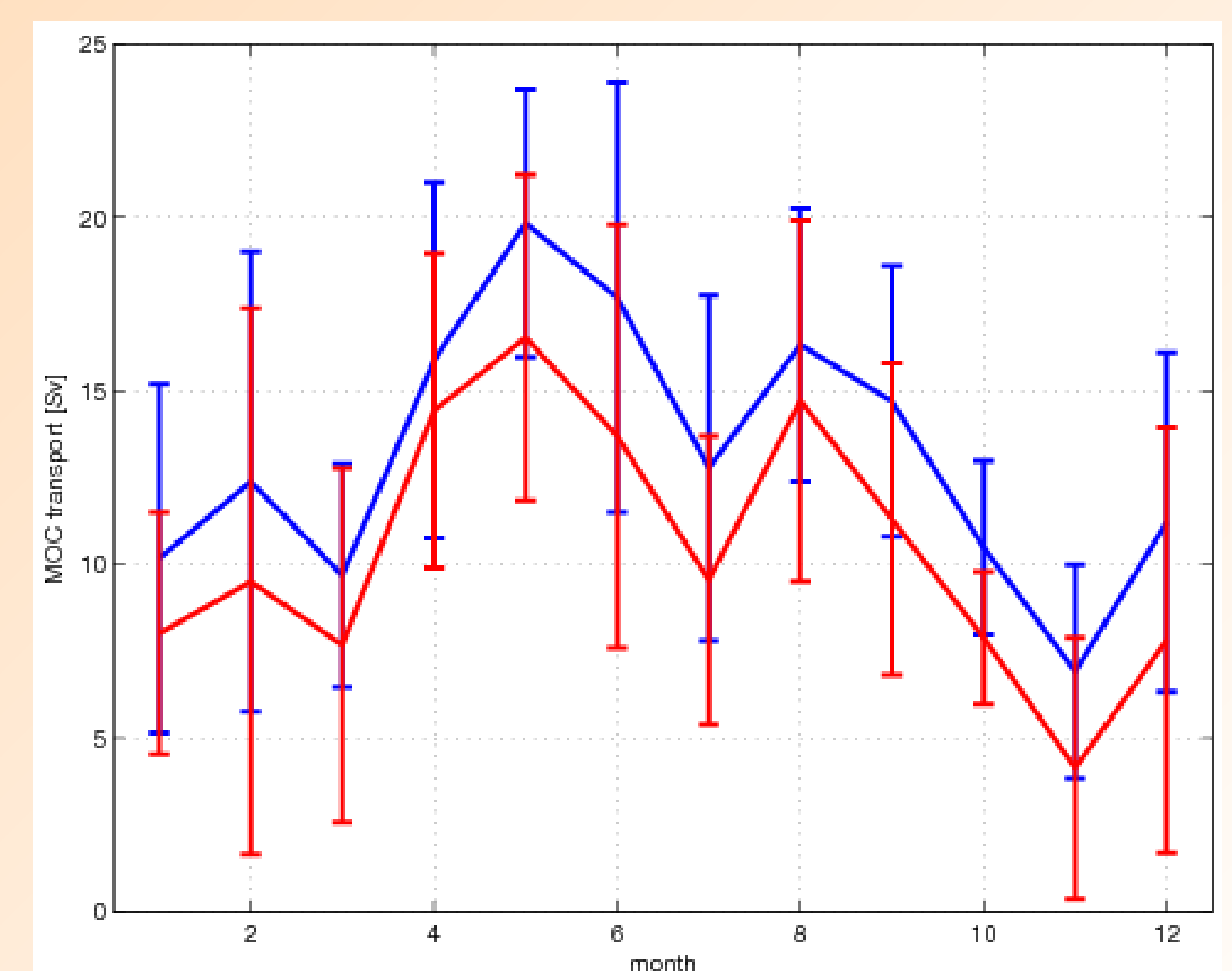


Fig. 3: Seasonal cycle of MOC transports at 35°S from HYCOM/NCODA (based on 48 monthly fields). Blue: full zonal resolution (0.08°). Red: reduced zonal resolution (0.5°). [unit: $1 \text{ Sv} = 10^6 \text{ m}^3 \text{ s}^{-1}$]

4. Seasonal Variability of the MOC Transport at 35S

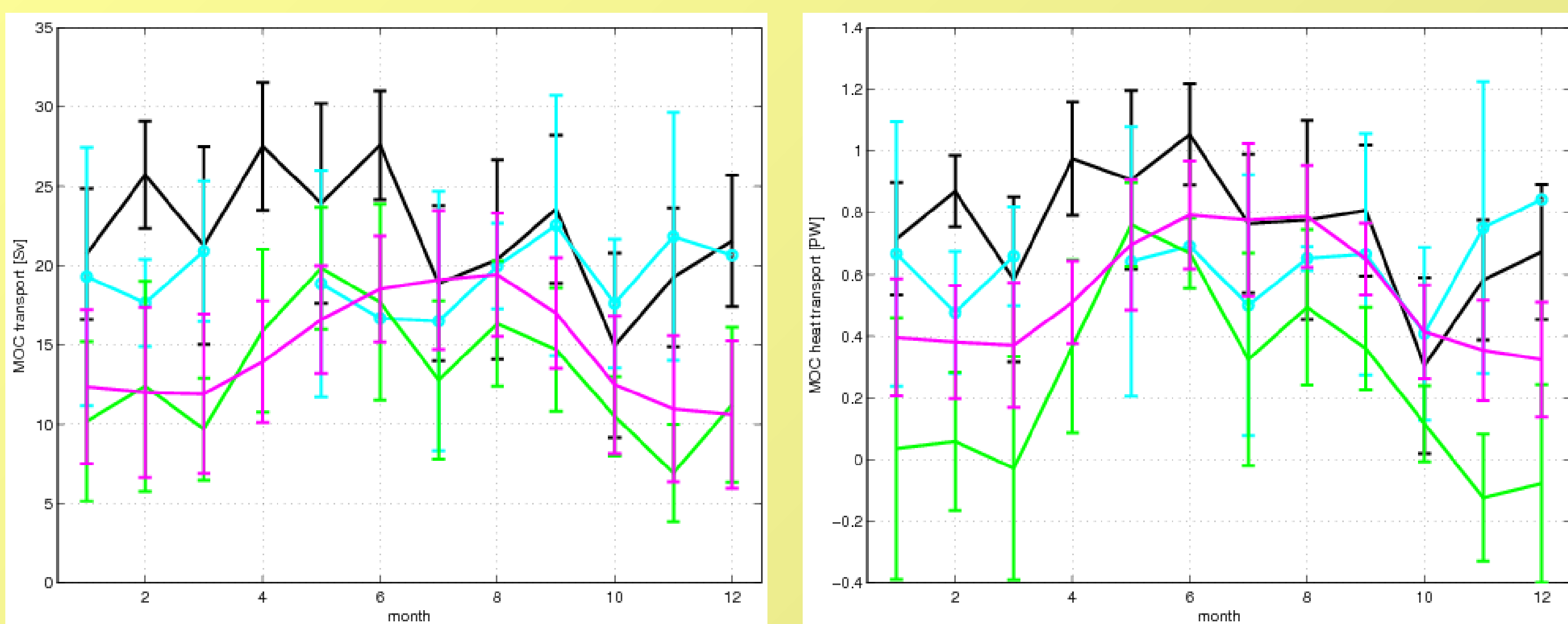


Fig. 4: Annual cycle of MOC volume (left) and heat (right) transports. Black: from Argo & SSH (35°S from 162 monthly mean sections), cyan: AX18 (nominally 35°S , 34 sections), magenta: NCEP/GODAS (35°S , from 151 monthly mean sections), green: HYCOM/NCODA (35°S from 48 monthly mean fields). Error bars represent standard deviations. [units: $1 \text{ Sv} = 10^6 \text{ m}^3 \text{ s}^{-1}$, $1 \text{ PW} = 10^{15} \text{ Watt}$]

The volume and heat transports of the MOC at 35°S reveal a weak seasonality (Fig. 4). The Argo&SSH data set (black lines) indicates that the transports are highest in April-June and lowest in October. The AX18 data set (cyan lines) does not reveal such a seasonality for two main reasons: (1) most monthly estimates are based on three or fewer transects (for Argo&SSH, the number of estimates per month is at least 13); (2) the XBT transects are often not at 35°S . NCEP/GODAS (magenta lines) and HYCOM/NCODA (green lines) also reveal seasonal cycles, but the peaks are not in the same months as for Argo&SSH. For HYCOM/NCODA, the maximum is found in May (in agreement with Argo&SSH) and the minimum occurs in November (one month later than in ARGO&SSH). For NCEP/GODAS the transports are highest in June to August and the minimum is found in December (i.e., roughly two months later than in Argo&SSH).

For all data sets the standard deviations of the monthly estimates are large, which is in general agreement with an earlier conclusion by Dong et al (2009) that the MOC variability is not dominated by a seasonal cycle.

With respect of the magnitude of the annual mean transports, the observational estimates agree quite well with each other ($19 \pm 2 \text{ Sv}$, $0.6 \pm 0.1 \text{ PW}$ for the AX18 versus $22 \pm 4 \text{ Sv}$, $0.8 \pm 0.2 \text{ PW}$ for Argo&SSH). NCEP/GODAS is quite close to the observations ($15 \pm 3 \text{ Sv}$, $0.5 \pm 0.2 \text{ PW}$), while the HYCOM/NCODA estimate is quite low ($10 \pm 4 \text{ Sv}$, $0.2 \pm 0.3 \text{ PW}$).

5. Long-term Variability of the MOC Transport at 35S

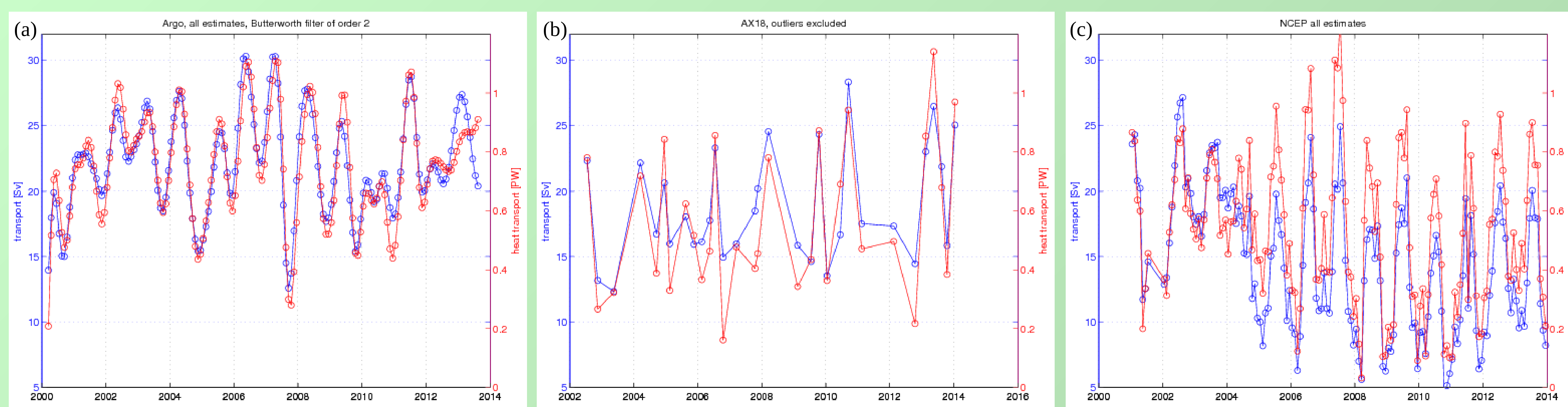


Fig. 5: Long-term variability of MOC volume (blue) and heat (red) transports. (a) from Argo and SSH (35°S , 162 monthly mean sections), (b) from AX18 (nominally 35°S , 34 sections), (c) from NCEP/GODAS (35°S , from 151 monthly mean sections). [units: $1 \text{ Sv} = 10^6 \text{ m}^3 \text{ s}^{-1}$, $1 \text{ PW} = 10^{15} \text{ Watt}$]

In the full time series (Fig. 5), the range of the observations-based estimates of the volume and heat transports is about 10-30 Sv and 0.2-1.1 PW, respectively. The range of values for the volume transports of NCEP/GODAS is shifted by about 5 Sv towards lower values.

As indicated above the mean seasonal cycle of the MOC transports is very weak. A look at the full time series reveals that there are large seasonal amplitudes, both in the estimates from Argo&SSH as well as in those based on NCEP, that vary strongly from year to year. In the AX18 data this pattern is not as clearly represented due to the smaller number of estimates.

It is interesting to note that matching periods of low and high amplitudes can be seen both in Argo&SSH and in NCEP/GODAS (e.g., 2006-2008 has high amplitudes in both).